Schnaid F. (2009). *In Situ Testing in Geomechanics – the main tests*. Taylor & Francis Group, London: 327 p. Chapter 6. Flat Dilatometer testing (DMT) 242-272.

Chapter 6

Flat dilatometer test (DMT)

> In geotechnical design it has long been recognised that the assessment of soil properties is the most important single task. By comparison the details of numerical analyses are of much lesser consequence.
>
> (N. Janbu, 1985)

General considerations

The dilatometer consists of a stainless steel blade with a circular, thin steel membrane mounted flat on one face. The blade is driven vertically into the soil using pushing rigs adapted from those used in the CPT. Penetration is halted every 20 cm and a test is performed by inflating the membrane and taking a series of pressure readings at prescribed displacements. The test is suitable for a wide variety of soils such as clay, sand, silt and hard formations. While the flat dilatometer test (DMT) is a commercial tool used worldwide in geotechnical investigation, only relatively recently have attempts been made to establish guidelines for good practice and to gain a more systematic understanding of interpretation and design applications. Understandably, this recent progress coincides with increasing acceptance of the DMT as a routine site investigation tool.

The DMT was developed in Italy by Silvano Marchetti in 1980. It is recognized here that Marchetti's efforts were of a pioneering nature and subsequent works on this subject followed his original basic conceptual framework. From a historical point of view, the DMT was conceived to establish a reliable operational modulus for the problem of laterally loaded piles (Marchetti, 2006). Later, the interpretation of test results was extended to provide measurements of in situ stiffness, strength and stress history of the soil. The equipment, test method and original correlations described by Marchetti (1980) were the essential initial steps towards establishing a procedure capable of supporting geotechnical applications.

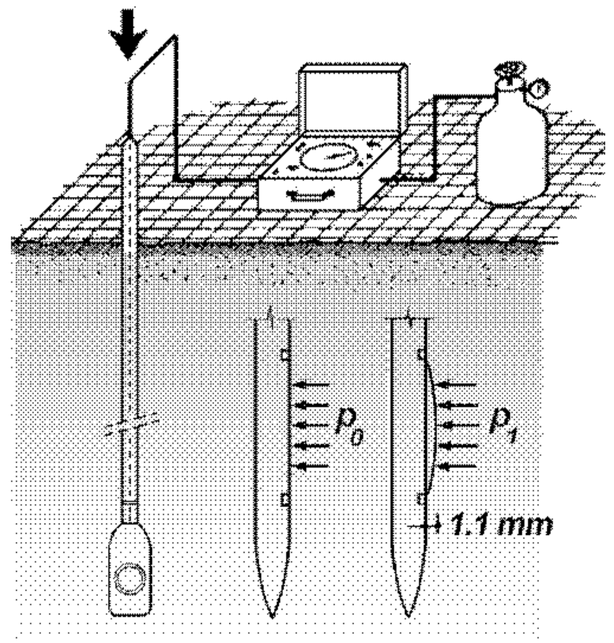

Figure 6.1 Schematic representation of the dilatometer test (Marchetti *et al.*, 2001).

Comprehensive assessments of the state of the art of DMT in research and practice were made by Lunne *et al.* (1989), Lutenegger (1988) and Marchetti (1997). In 2001, a report was issued under the auspices of the ISSMGE Technical Committee TC 16 (Ground Property Characterisation from *In Situ* Testing) by Marchetti *et al.* (2001). The increasing interest in the subject gave rise to a number of specific conferences – the 1st International Conference on the Flat Dilatometer (Canada, 1993), International Seminar on the Flat Dilatometer and its Applications to Geotechnical Design (Tokyo, 1999) and, most recently, the 2nd International Conference on Flat Dilatometer Testing (Washington, 2006). A research project sponsored by the Federal Highway Administration (FHWA) produced a practical manual designed to encourage the use of the DMT in the USA (Schmertmann, 1988). In addition to these contributions, a large number of key publications established a body of practical references on the DMT (e.g. Lacasse and Lunne, 1986; Robertson *et al.*, 1987; Powell and Uglow, 1988; Marchetti and Totani, 1989; Kamey and Iwasaki, 1995; Mayne *et al.*, 1999).

Equipment and procedures

The dilatometer is illustrated schematically in Figure 6.1, showing the control unit, dilatometer blade, push rods and gas tank. Figure 6.2 shows the DMT set up with a control unit that typically includes a pair of pressure

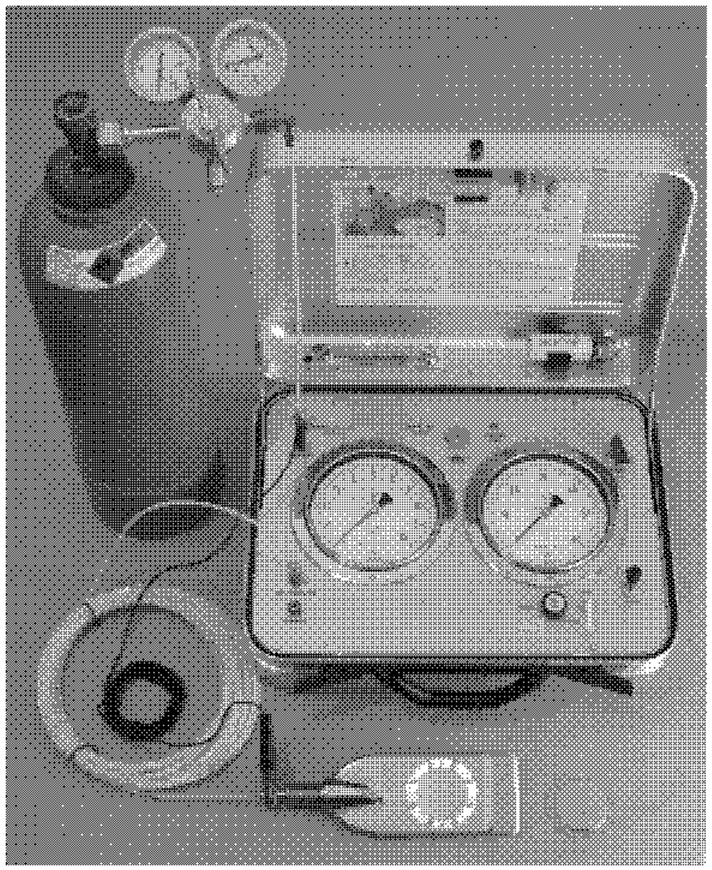

Figure 6.2 The flat dilatometer (courtesy of Marchetti).

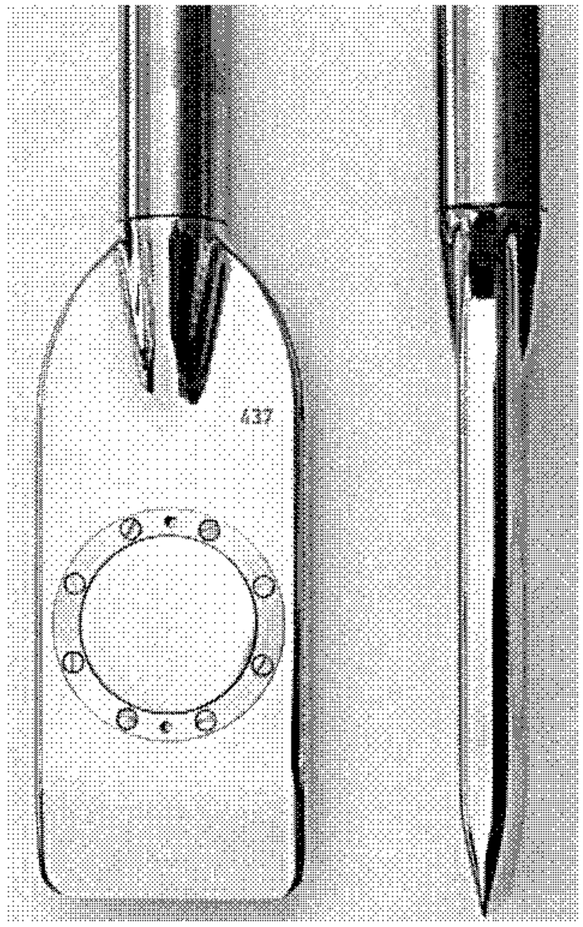

Figure 6.3 The flat dilatometer blades – front and side views (courtesy of Marchetti).

gauges (for low-range (1 MPa) and high-range (6 MPa) measurements), valves for controlling gas flow, a galvanometer and audio buzzer signal.

The dilatometer steel blade front and side views are shown in Figure 6.3. Nominal dimensions of the blade are 95 mm width and 15 mm thickness, having a cutting edge angled between 24° and 32° to penetrate the soil. The blade is designed to safely withstand up to 250 kN pushing force. Also shown in Figure 6.3 is the 60 mm dia. and 0.20 mm thick circular steel membrane that is connected to the blade by a retaining ring. Figure 6.4 illustrates the design features of this membrane, which protects a sensing disc that is stationary at rest and kept in position press-fitted inside the insulating seat. The insulation prevents any electrical contact with the steel body of the dilatometer (Figure 6.5). The blade is connected to a control unit by a pneumatic-electrical tube capable of transmitting a combined gas pressure and electrical signal.

The test starts by driving the blade into the soil at a constant rate, generally between 10 and 20 mm/s. After penetration, the membrane is inflated through the control unit and a sequence of pressure readings is made at prescribed displacements, corresponding to:

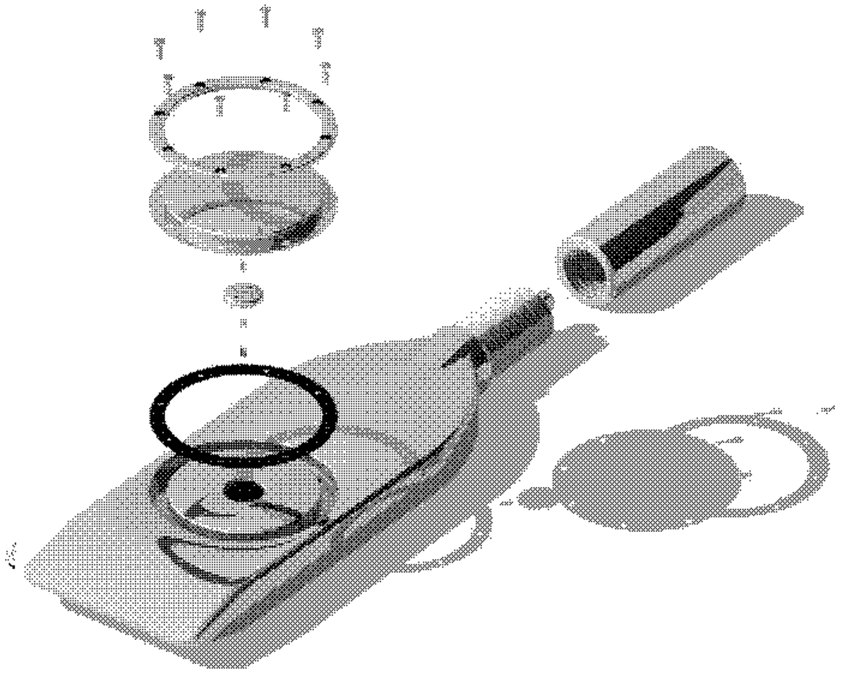

Figure 6.4 The flat dilatometer membrane (courtesy of Marchetti).

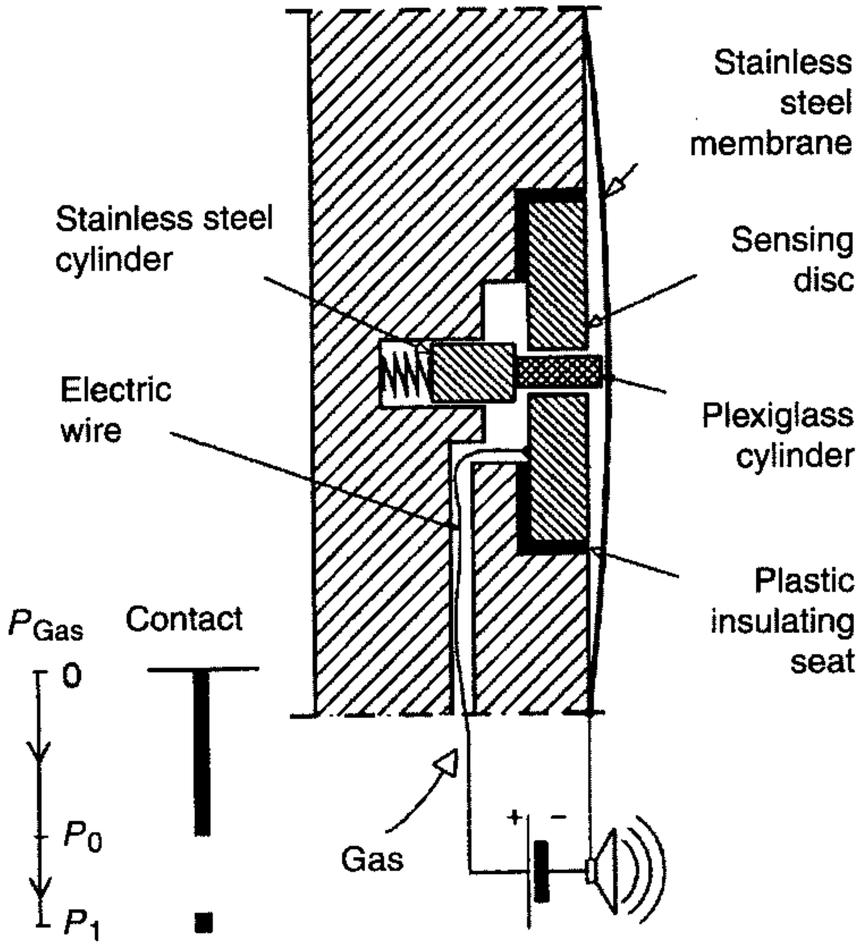

Figure 6.5 DMT working principle (Marchetti *et al.*, 2001).

1 the *A*-pressure at which the membrane starts to expand ('lift-off');
2 the *B*-pressure required to move the centre of the membrane by 1.1 mm against the soil;
3 the optional *C*-pressure, or closing pressure, taken by slowly deflating the membrane soon after the *B*-reading. The rationale behind this measurement is that, in sand, as the membrane deflates the closing pressure approximately equals the pressure of the water u_0.[1]

Before expansion, the sensing disc is grounded and the control unit emits a continual beeping sound. When the internal pressure slightly exceeds the external soil horizontal stress, the membrane starts to move, losing the electrical contact and cutting off the signal. This signal is reactivated when the centre of the membrane has moved 1.1 mm and the spring-loaded steel cylinder touches the inner face of the sensing disc. Deactivation and reactivation

of the signal prompts the operator to take the *A* and *B* pressure readings respectively. Despite its simplicity, this working system has proved to be fairly accurate and reliable. Furthermore, the fact that results were highly reproducible was fully acknowledged by investigators and practitioners.

Once the process described above is complete and the membrane is fully deflated, the operator advances the blade to a new desired depth and repeats the test. The time delay between the end of the pushing stage and the start of inflation is no more than a few seconds. Eurocode 7 (1997) recommends that the rate of inflation shall be such that the *A*-reading is obtained within 20 s after reaching the test depth and the *B*-reading within 20 s after the *A*-reading. Each test sequence typically requires around 1 min. Tests carried out within the above limits give, essentially, a drained response in sand and an undrained response in clay. In intermediate permeability silty soils partial drainage conditions may occur which impact our ability to interpret test results.

As recognized by Marchetti and Crapps (1981) and Marchetti (1999), calibrations for membrane stiffness are an essential operation to obtain the corrected pressures during the expansion and contraction phases and they have an appreciable influence on the measured soil parameters derived from test results. Calibration consists of correcting the *A* and *B* readings for membrane stiffness to obtain:

- ΔA = external pressure that must be applied to the membrane in free air to guarantee a perfect contact against its seating (i.e. *A*-position);
- ΔB = internal pressure which in free air lifts the membrane centre 1.1 mm from its seating (i.e. *B*-position).

ΔA and ΔB can be measured by a simple procedure using the control unit and a syringe to generate vacuum or pressure. As a basic rule, this procedure must be carried out before and after each sounding, especially in soft soils where *A* and *B* are small numbers, of the order of magnitude of the membrane stiffness. These calibrations should fall within the tolerances given by Eurocode 7 (EN ISO 22476-5) which recommends that, before inserting the blade, the initial readings of ΔA must be within the range of 5 to 30 kPa and ΔB within the range of 5 to 80 kPa. Any membrane that fails to meet these recommendations should be replaced. In order to fall within the range of valid readings, the change of ΔA or ΔB must not exceed 25 kPa at the end of the sounding.

Values of ΔA and ΔB are used to correct the *A* and *B* readings respectively in order to determine the pressures p_0 and p_1 from the following expressions:

$$p_0 = 1.05(A - Z_m + \Delta A) - 0.05(B - Z_m - \Delta B) \tag{6.1}$$

$$p_1 = (B - Z_m - \Delta B) \tag{6.2}$$

where Z_m is the gauge zero offset when vented to atmospheric pressure.

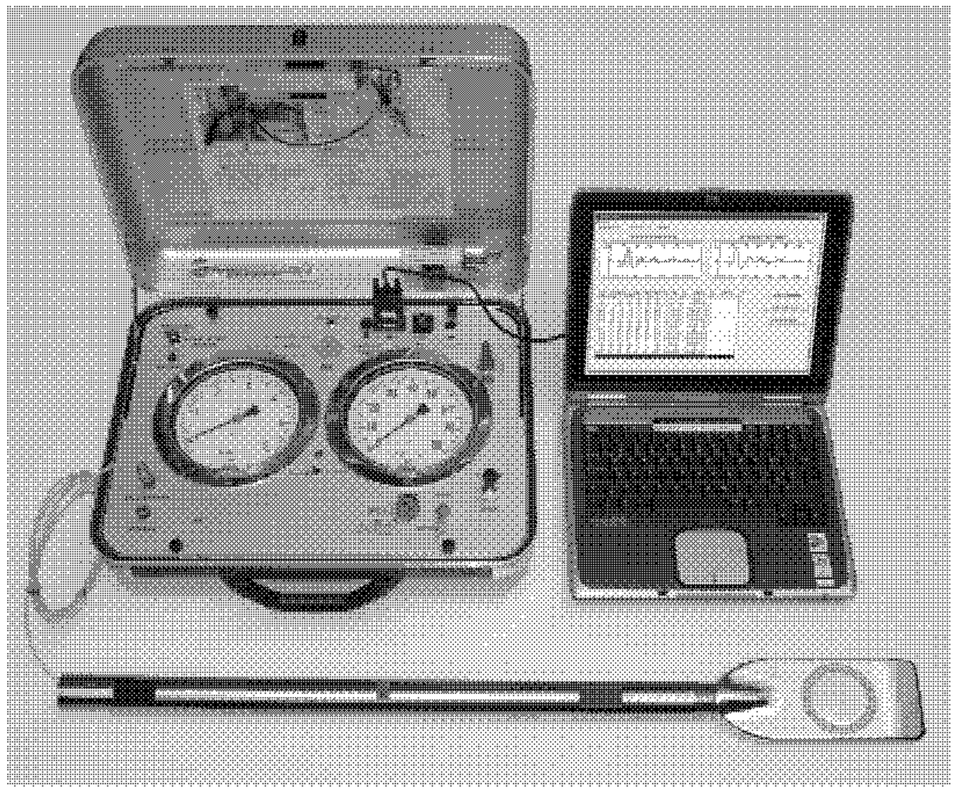

Figure 6.6 The seismic dilatometer (courtesy of Marchetti).

The calculated pressures p_0 and p_1 are subsequently used for interpretation of DMT results in the assessment of soil constitutive parameters. The p_0 pressure is inherently related to the in situ horizontal effective stress and therefore also related to the preconsolidation pressure and stress history. The difference between p_0 and p_1 forms the basis for evaluating soil compressibility.

A relatively recent development (Figure 6.6), the seismic dilatometer (SDMT) is a combination of the standard flat dilatometer (DMT) with a seismic module (Hepton, 1988; Martin and Mayne, 1997; Mayne *et al.*, 1999). This module houses two receivers spaced 0.5 m apart for measuring the shear wave velocity v_s from which the small strain shear modulus G_0 can be determined (see Chapter 3 under Seismic cone):

$$G_0 = \rho(v_s)^2 \qquad (3.1)\text{idem}$$

where ρ is the mass density. There are important benefits of including the v_s reading (and G_0) with a standard dilatometer. An independent measurement of soil stiffness enhances our ability to solve problems, such as the

seismic behaviour of sandy soils during earthquakes and soil–structure interaction response under dynamic loads.

Intermediate DMT parameters

Interpretation of the DMT is based predominantly on empirical correlations related to three index parameters: material index, horizontal stress index and dilatometer modulus.

Material index I_D

The material index I_D is defined as:

$$I_D = \frac{p_1 - p_0}{p_0 - u_0} \qquad (6.3)$$

where u_0 is the hydrostatic porewater pressure. The material index provides a reasonable estimate of soil type and was introduced by Marchetti (1980) after the observation that the difference between p_0 and p_1 is small for clay and large for sand.

Horizontal stress index K_D

The horizontal stress index K_D is expressed as:

$$K_D = \frac{p_0 - u_0}{\sigma'_{v0}} \qquad (6.4)$$

where σ'_{v0} is the in situ vertical effective stress. K_D can be regarded as K_0 amplified by the penetration of the blade. Two experimental results are observed in clay deposits: in normally consolidated, uncemented clay the value of K_D is approximately 2 and the K_D profile is similar in shape to the OCR profile, giving an indication of the variation of the stress history of the soil with depth.

Dilatometer modulus E_D

The dilatometer modulus is obtained by relating the displacement s_0 to p_0 and p_1 using the theory of elasticity (Gravesen, 1960). The solution assumes that:

- the space surrounding the dilatometer is formed by two elastic half-spaces, in contact along the plane of symmetry of the blade; and
- zero settlement is computed externally to the loaded area:

$$s_0 = \frac{2D(p_1 - p_0)}{\pi}\frac{(1 - \nu^2)}{E} \qquad (6.5)$$

where E is Young's modulus and ν Poisson's ratio. For a membrane diameter D equal to 60 mm and a displacement s_0 equal to 1.1 mm, equation (6.5) approaches:

$$E_D = 34.7(p_1 - p_0) \tag{6.6}$$

Although E_D is inherently an operational Young's modulus (both E and E_D are calculated using elastic theory), it is recognized that the expansion of the membrane from p_0 and p_1 reflects the disturbed soil properties around the blade produced by DMT penetration.

Interpretation of test results

DMT interpretation methods are essentially based on correlations obtained by calibrating DMT pressure readings against thoroughly verified parameters (e.g. Marchetti, 1980, 1997; Lutenegger, 1988; Lunne *et al.*, 1989). These correlations are supported by experience, which shows that DMT parameters can be related to soil type, soil unit weight, coefficient of earth pressure at rest (K_0), overconsolidation ratio (OCR), constrained modulus (M), undrained shear strength (s_u) and friction angle (ϕ'). Given the empirical nature of the interpretation methods, existing correlations are, at least in part, site-specific and some scatter is expected between estimated and predicted values.

Substantial effort has been expended on the validation of DMT correlations. Given the physical constraints of modelling a dilatometer, closed-form solutions have been obtained just under considerably simplified assumptions (e.g. Schmertmann, 1986; Roque *et al.*, 1988; Kim and Paik, 2006; Lutenegger, 2006; Lutenegger and Adams, 2006). Finite element analysis should ideally model the penetration and the inflation of the membrane as a truly three-dimensional phenomenon, in contrast with the two-dimensional axisymmetric representation of cone penetration. Since this is not a simple task, only a limited number of reported numerical studies have tackled the problem of the numerical representation of boundary conditions around the blade (e.g. Baligh and Scott, 1975; Finno, 1993; Yu *et al.*, 1993; Smith and Houlsby, 1995; Yu, 2004; Balachowski, 2006). Important contributions will be reviewed throughout this chapter.

Soil characterization

Recommendations and requirements for the graphical presentation of DMT data are fairly basic. The information to be presented combines two DMT intermediate parameters (I_D and K_D) with two derived soil parameters (the constrained modulus M and the undrained shear strength s_u) that are displayed side by side in four profiles. Note that I_D gives a clear indication of soil type, whereas K_D gives an assessment of the stress history of the deposit

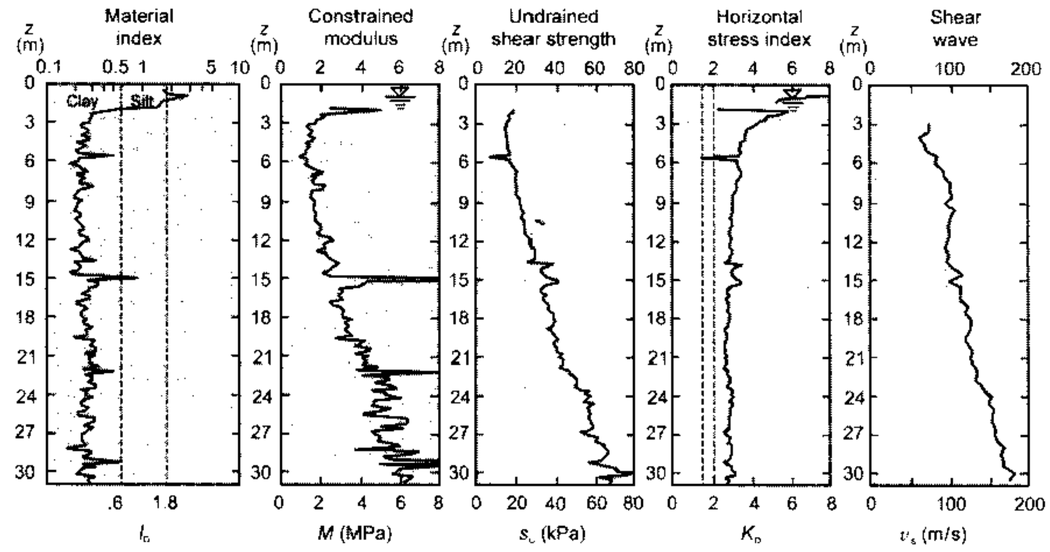

Figure 6.7 Typical SDMT in clay (Marchetti et *al.*, 2007).

by describing the shape of OCR with depth. For a seismic dilatometer, a fifth profile is added by displaying the shear wave velocity with depth.

Typical DMT profiles in clay and sand are shown in Figures 6.7 and 6.8, respectively. Figure 6.7 gives an example of the typical graphical representation of the SDMT-recorded output at the Futino clay research site (after Marchetti *et al.*, 2007). The output displays the profiles of the four basic DMT parameters, I_D (soil type), M, s_u and K_D (related to OCR), as well as the profile of v_s. Values of I_D fall consistently within the range of 0.1 to 0.5, which is characteristic of clay deposits. Both the constrained modulus and the undrained shear strength show a steady increase with increasing depth for values ranging from 2 to 6 MPa and 10 to 60 kPa, respectively. An interesting feature, which will be explored below, is the reduction of K_D from the surface to a relatively uniform value of $K_D = 2$. Since K_D profiles generally reflect OCR, this pattern would indicate a desiccated OC crust near the surface overlying a normally consolidated clay.

SDMT results at the Catania site in Italy are shown in Figure 6.8 to illustrate the DMT response in sand (Maugeri and Monaco, 2006). Values of I_D, M and K_D are fairly uniform at values of 2, 200 MPa and 5 respectively. The constrained modulus is much higher than values reported in the soft clay deposit at Futino, yielding a value of 200 MPa compared to the measured 5 MPa in clay. The shear velocity increases with depth, typically ranging from 200 m/s near the surface to about 300 m/s at 22 m depth.

Evidence of the consistency of test results has prompted the development of charts designed to identify soil type and estimate unit weight γ from I_D

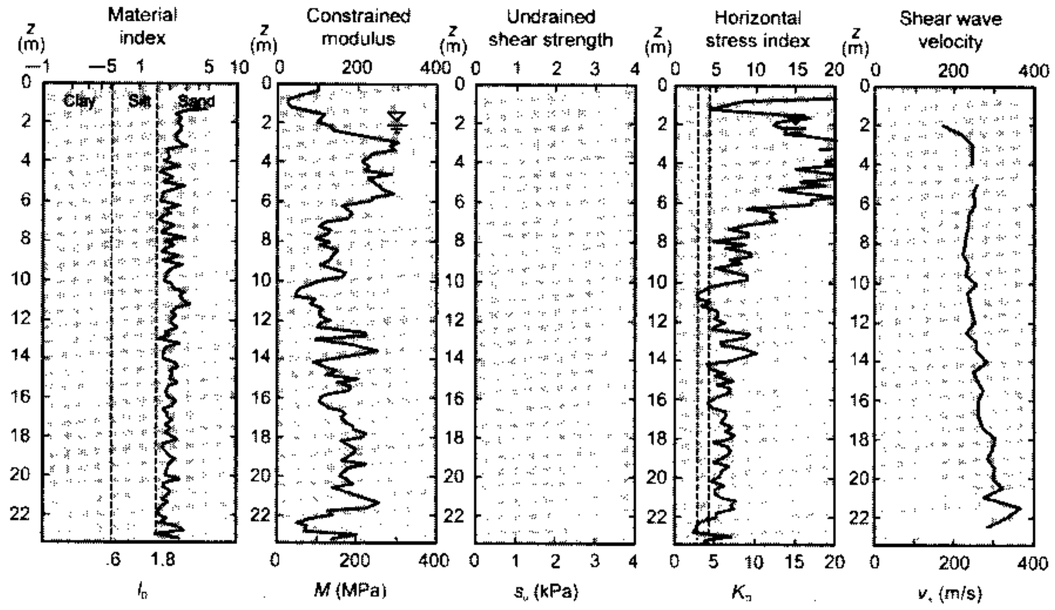

Figure 6.8 Typical SDMT in sand (Maugeri and Monaco, 2006).

and E_D (Marchetti and Crapps, 1981; Lacasse and Lunne, 1988), as illustrated in Figure 6.9. Charts of this type provide estimations of the sub-soil strata and the correspondent values of γ that are necessary to calculate σ'_{v0}.

Geotechnical parameters in clay

In clay, DMT data can provide direct assessment of the overconsolidation ratio, coefficient of earth pressure at rest, undrained shear strength, soil stiffness and coefficient of consolidation.

Overconsolidation ratio (OCR)

The similarity between the dilatometer K_D and OCR profiles was first pointed out by Marchetti (1980) and later confirmed by several authors (e.g. Jamiolkowski *et al.*, 1988; Powell and Uglow, 1988; Kamey and Iwasaki, 1995). For uncemented clays, OCR can be predicted to be:

$$OCR = (0.5K_D)^{1.56} \tag{6.7}$$

which is consistent with the experimental evidence that $K_D \approx 2$ for $OCR = 1$. The usefulness of this approach has been demonstrated experimentally by Kamey and Iwasaki (1995), as illustrated in Figure 6.10. Although a small variation in the coefficients in equation (6.7) may be acceptable to match local conditions, there is sufficient evidence to suggest that K_D profiles are

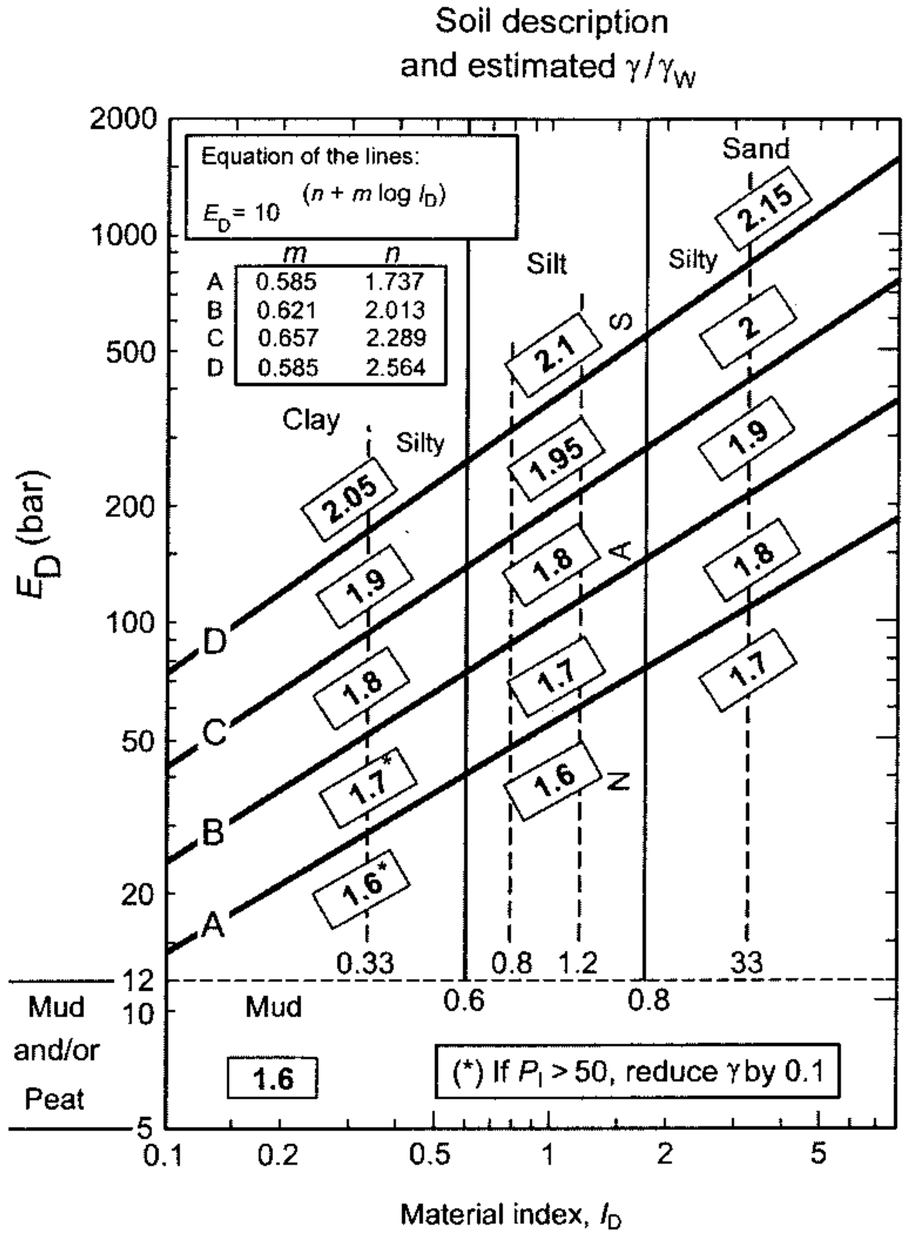

Figure 6.9 Chart for estimating soil type and unit weight (Marchetti and Crapps, 1981).

helpful in characterizing the stress history of the soil, allowing NC and OC clay deposits to be recognized and desiccated crusts to be identified.

Assuming that the installation of a flat dilatometer can be simulated by a flat cavity expansion process, Yu (2004) produced a sound numerical validation of the K_D and OCR relationship (Figure 6.11). The comparison between numerical simulations and the empirical correlation suggests that equation (6.7) can be used with reasonable confidence in most conditions, with the exception of heavily overconsolidated clays ($OCR > 8$).

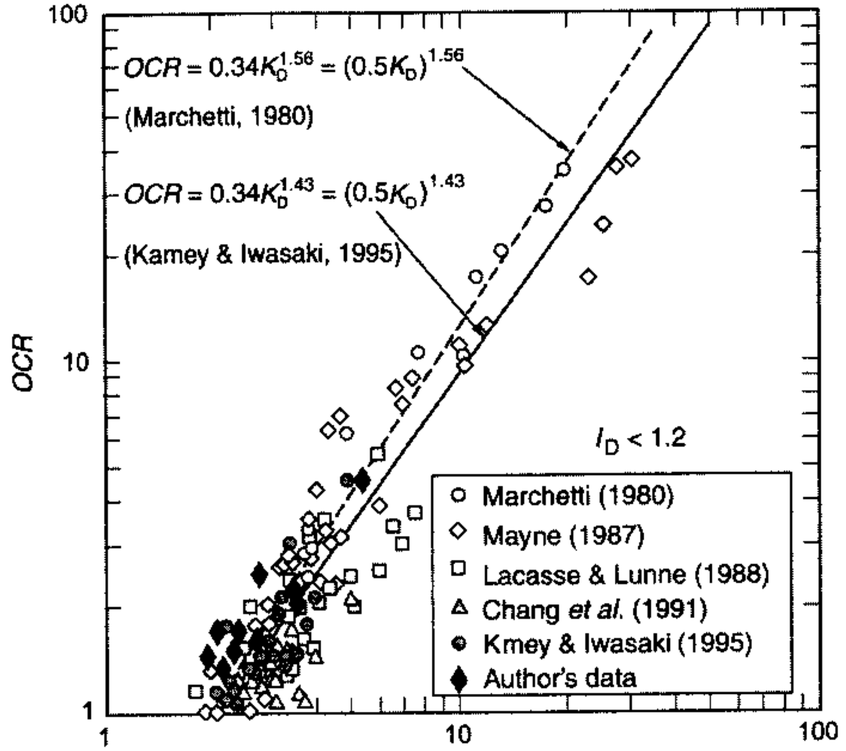

Figure 6.10 Correlations of K_D and *OCR* for cohesive soils (modified from Kamey and Iwasaki, 1995).

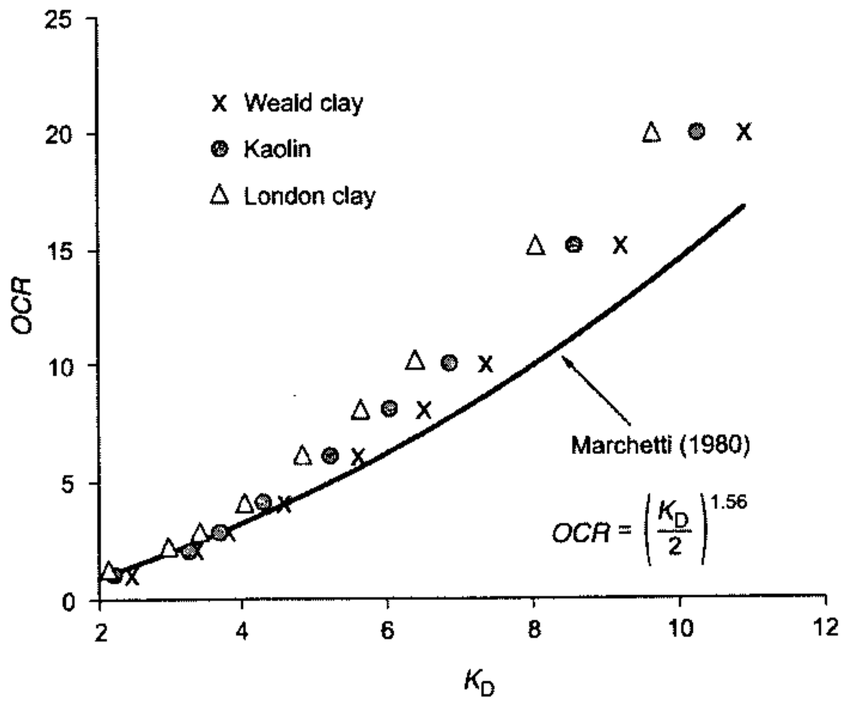

Figure 6.11 Theoretical correlation between K_D and *OCR* (Yu, 2004).

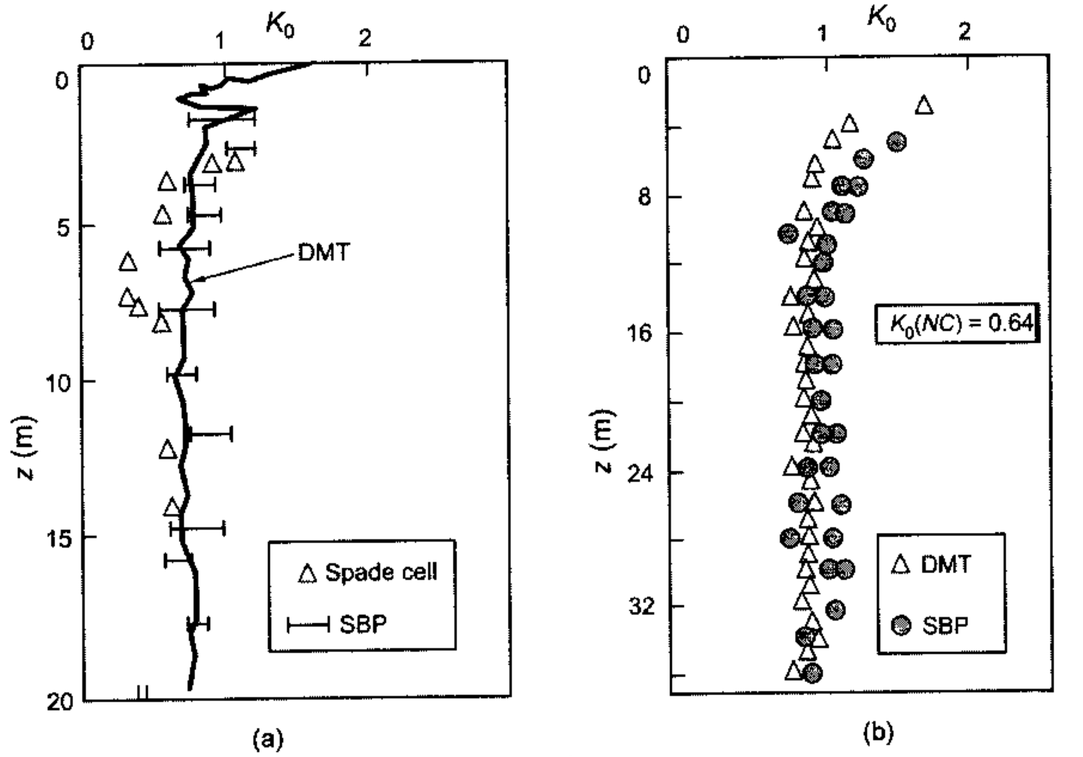

Figure 6.12 Comparison between K_0 values derived from DMT and self-boring pressuremeter (SBP) results at (a) Bothkennar research site (Nash *et al.*, 1992) and (b) Fucino research site (Burghignoli *et al.*, 1991).

As already recognized by Marchetti *et al.* (2001), equation (6.7) is not applicable to structured (cemented) materials. Soil structuration produces an increase in K_D, whereas soil destructuration, produced by driving the blade into the soil, would produce an opposite effect. The magnitude of these effects depends on the nature of the cementing agent and, for this reason, a standardized K_D–*OCR* correlation cannot be achieved.

Coefficient of earth pressure at rest

Several attempts have been made to correlate the coefficient of earth pressure at rest K_0 to the horizontal stress index K_D in uncemented clay (Marchetti, 1980; Lacasse and Lunne, 1988; Powell and Uglow, 1988; Kulhawy and Mayne, 1990). These correlations give the same broad information as that derived from Marchetti's original equation (1980):

$$K_0 = \left(\frac{K_D}{1.5}\right)^{0.47} - 0.6 \tag{6.8}$$

In Figure 6.12, it can be seen that, for the dilatometer, the deduced K_0 values are very close to K_0 values derived from the self-boring pressuremeter

at the two research sites of Bothkennar (Nash *et al.*, 1992) and Fucino (Burghignoli *et al.*, 1991). Numerical work carried out by Yu (2004) shows that, although K_0–K_D relationships are sensitive to critical state parameters, equation (6.8) generally gives a reasonable estimation of K_0 in clay.

Undrained shear strength

The dependence of normalized undrained shear strength s_u/σ'_{v0} on OCR is well-known and has been extensively discussed throughout this book (see Chapters 2 and 3). The K_D versus OCR correlation has therefore prompted investigations into possible relations between K_D and s_u/σ'_{v0} and, consequently, the development of correlations to estimate s_u (Marchetti, 1980; Lacasse and Lunne, 1988; Powell and Uglow, 1988). The original correlation, as proposed by Marchetti (1980), is:

$$s_u = 0.22\sigma'_{v0}(0.5K_D)^{1.25} \tag{6.9}$$

Numerical analysis of the installation of flat dilatometers reported by Huang (1989), Finno (1993), Whittle and Aubeny (1993) and Yu (2004) generally supports the s_u–K_D correlation from equation (6.9) (e.g. Marchetti, 1980; Marchetti *et al.*, 2001). Case studies comparing s_u values determined from the dilatometer with those obtained from other testing techniques have been presented by Lacasse and Lunne (1988), Powell and Uglow (1988), Burghignoli *et al.* (1991), Iwasaki *et al.* (1991), Nash *et al.* (1992), Coutinho *et al.* (1998) and others. The results of several reported cases are compiled in Figure 6.13.

Soil stiffness

Several attempts have been made to correlate the DMT intermediate parameters to soil stiffness, from which the constrained modulus, Young's modulus and small strain shear modulus can be assessed. Marchetti's original work in the 1980s has already explored this possibility by correlating the constrained modulus M and E_D in the form:

$$M_{DMT} = R_M E_D \tag{6.10}$$

where R_M is an empirical coefficient that ranges mostly between 1 and 3 and is known to be sensitive to I_D. The equations expressing R_M are:

$$\begin{aligned}
&\text{if } I_D \le 0.6 && R_M = 0.14 + 2.36\ \log K_D \\
&\text{if } I_D \ge 0.3 && R_M = 0.5 + 2\ \log K_D \\
&\text{if } 0.6 < I_D < 3 && R_M = R_{M0} + (2.5 - R_{M0})\log K_D \\
& && \text{with } R_{M0} = 0.14 + 0.15(I_D - 0.6) \\
&\text{if } K_D > 10 && R_M = 0.32 + 2.18\ \log K_D \\
&\text{if } R_M < 0.85 && \text{set } R_M = 0.85
\end{aligned} \tag{6.11}$$

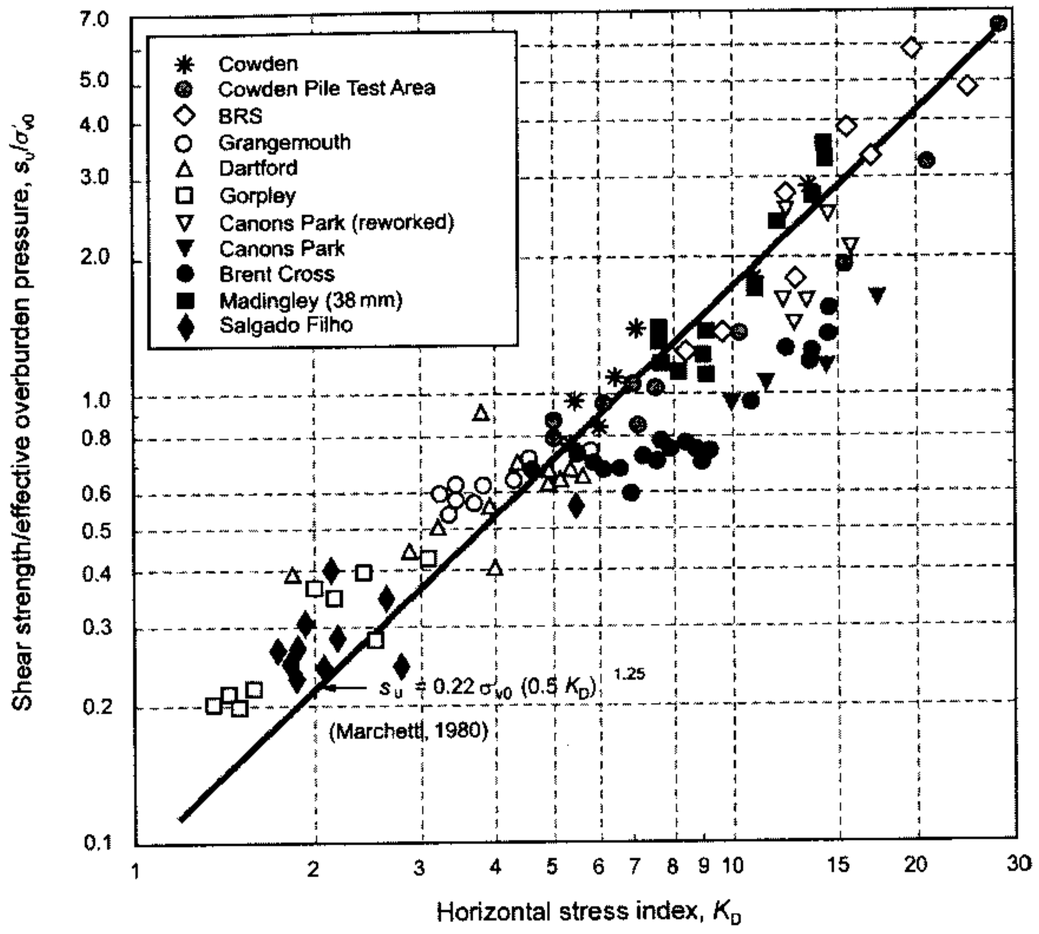

Figure 6.13 Undrained shear strength from dilatometer (modified from Powell and Uglow, 1988).

Given the nature of the correlated parameters, and because a vertical *drained* confined modulus cannot be expected to correlate to an *undrained* horizontal cavity expansion modulus, scatter in R_M is expected. In addition, although soil stiffness is known to be largely controlled by soil stress history, E_D does not reflect this dependency. Despite due recognition of these limitations, experience has generally shown that the DMT provides an indication of M (Figure 6.14) and consequently yields some useful predictions of settlements in clay deposits.

The drained Young's modulus can be derived directly from M_{DMT} using elastic theory:

$$E' = \frac{(1+\nu)(1-2\nu)}{(1-\nu)}M \tag{6.12}$$

bearing in mind that a Poisson's ratio of 0.25 gives $E' \approx 0.8M_{DMT}$.

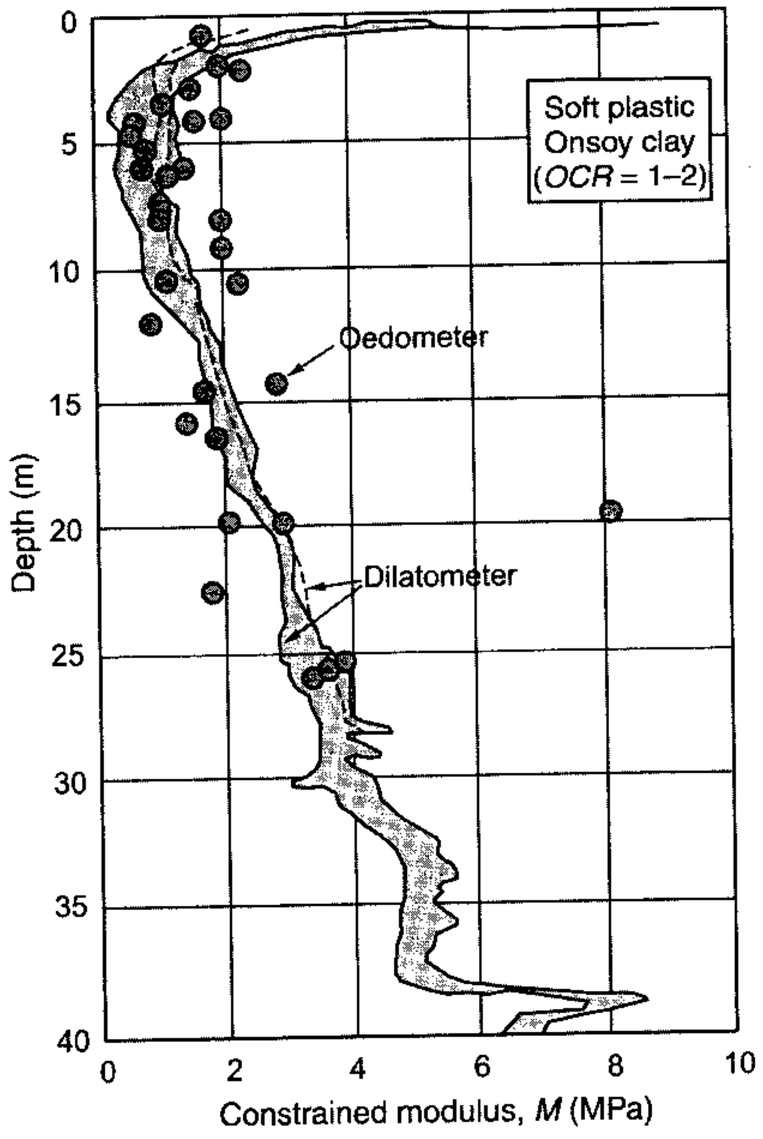

Figure 6.14 Comparison between *M* determined by DMT and by high-quality oedometer results (Lacasse, 1986).

Recently, attempts have been made to estimate the small strain shear modulus G_0 from E_D (Lunne *et al.*, 1989; Hryciw, 1990; Tanaka and Tanaka, 1998):

$$G_0/E_D = 7.5 \text{ for normally consolidated clays} \qquad (6.13)$$

This equation is subject to the restrictions discussed throughout this book and, given the facilities available to measure G_0 from shear wave velocities, the use of a seismic dilatometer is recommended for this purpose.

Coefficient of consolidation

In low permeability soils, the excess pore pressure induced by the penetration of the blade dissipates much more slowly than the pressure induced by the DMT test. Since the dilatometer does not measure the environmental pore pressure, an assumption is made that the flow parameter can be assessed from the measured decay with time of a dilatometer reading (A or C). Three methods are currently used for dissipation tests: DMT-A method (Marchetti and Totani, 1989), DMT-A2 method (Schmertmann, 1988) and DMT-C method (Robertson *et al.*, 1988). Whereas the A and A2 methods monitor contact horizontal stress, the C method records the closing pressure (known to converge with the in situ equilibrium pore pressure).

Interpretation procedures are fairly similar in all methods. For this reason, only the DMT-A method is detailed in this book (Marchetti *et al.*, 2001):

1 plot the A-log *t* DMT curve;
2 identify the contraflexure point in the curve (as represented in Figure 6.15) and the associated time (t_{flex});
3 obtain C_h from the following equation:

$$C_h(OC) = \frac{7cm^2}{t_{flex}} \qquad (6.14)$$

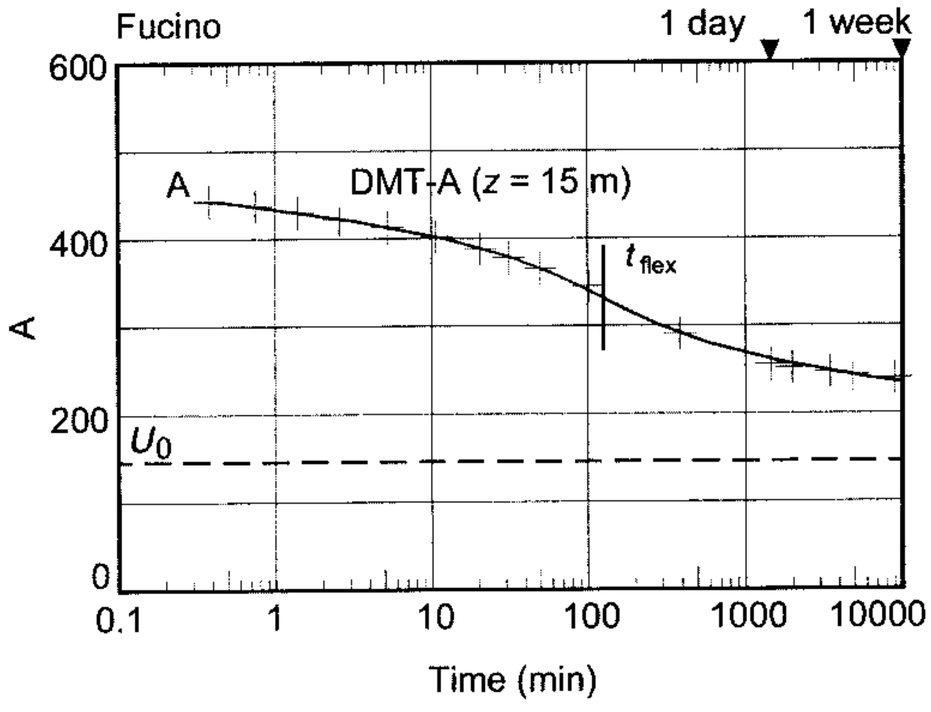

Figure 6.15 Coefficient of consolidation (Marchetti *et al.*, 2001).

Note that the value of C_h, estimated from equation (6.14), corresponds to soil behaviour in the overconsolidated range. As discussed in Chapter 3 under the heading Consolidation coefficients, a much lower C_h value should be used for estimating the rate of settlements in normally consolidated soils.

Geotechnical parameters in sand

In sand, both shear strength and stiffness can be assessed directly from measured DMT readings.

Friction angle

Prediction of the friction angle ϕ' in sand is primarily based on the evidence that the thrust necessary to push the dilatometer blade can be estimated directly from p_0 (and therefore from K_D, which is just a normalization of p_0 with respect to the vertical effective stress). Derived from the proportionality between K_D and penetration resistance (and then to tip cone resistance), Schmertmann (1982) proposed a method to estimate ϕ' using the bearing capacity theory of Durgunoglu and Mitchell (1975) already described in Chapter 3. This approach was later adapted by Marchetti (1985) in a graphical representation (Figure 6.16) that enables ϕ' to be estimated from K_0 and q_c or K_D. Since the value of K_0 is not easily determined, the author uses the values of the coefficients of earth pressure K_a and K_p and the previously mentioned Jacky's equation ($K_0 = 1 - \sin \phi'$) as reference to help in the decision-making process of selecting representative friction angles in sites where little geotechnical site information is available.

This basic empirical approach relies on the measured K_D from the DMT and requires an independent rough evaluation of K_0. A recent numerical analysis presented by Yu (2004) offered an instructive alternative approach to interpretation of DMTs in sand by demonstrating that, although K_D (or normalized K_D/K_0) increases with soil friction angle, the influence of the rigidity index (G_0/p'_0) is also highly significant. In the numerical analysis, the DMT has been modelled as a flat cavity expansion process using linear-elastic, perfectly-plastic Mohr-Coulomb theory. The study clearly identifies the need to take the rigidity index into account when estimating ϕ' values. In addition, it appears that, in a stiff soil, the displacement that originates with K_D is sufficiently small to be regarded as elastic; however, in a softer soil plastic strains may occur.

More recently, Marchetti (2001) made full use of the relationship between q_c and K_D to propose a method of estimating ϕ' directly from DMT K_D values:

$$\phi'_{DMT} = 28° + 14.6° \log K_D - 2.1° \log^2 K_D \qquad (6.15)$$

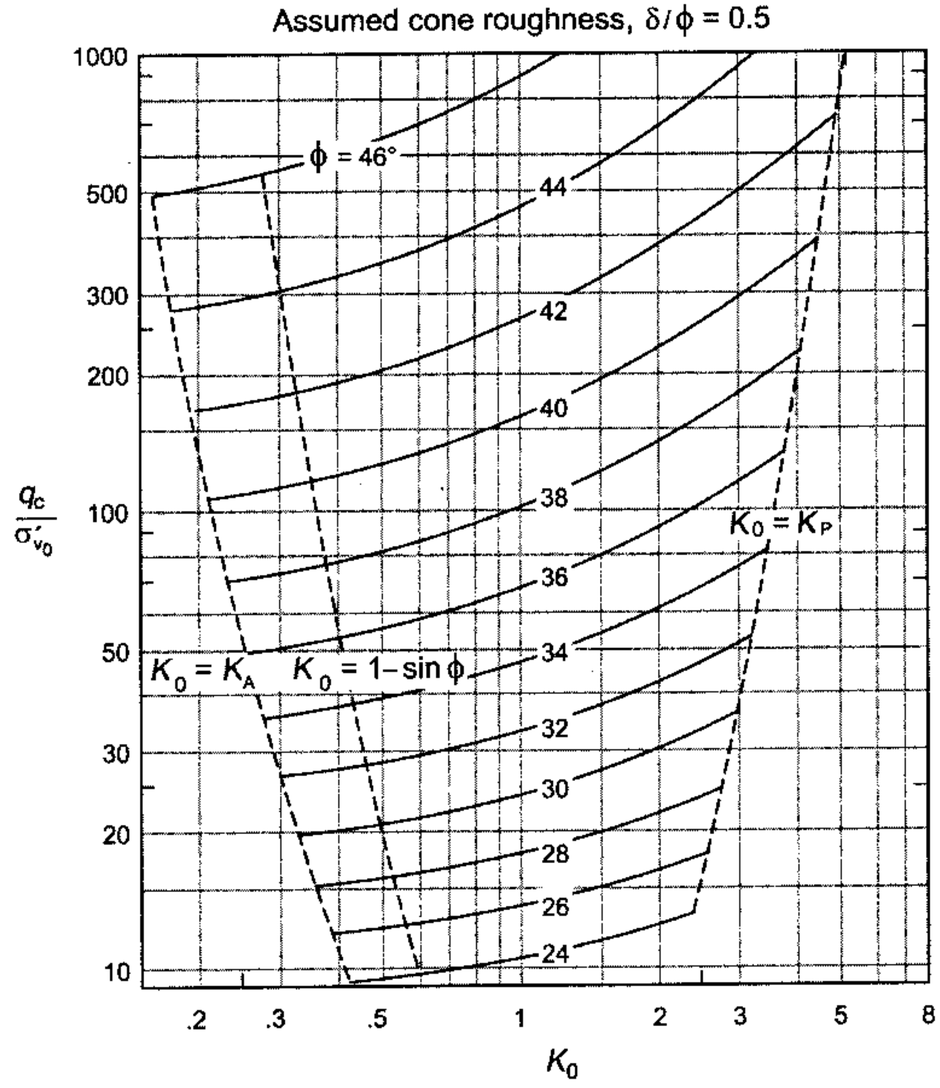

Figure 6.16 Graphical representation of q_c–K_0–ϕ' values (Marchetti, 1985).

Marchetti (2001) emphasizes that equation (6.15) is not intended to be an accurate estimation of ϕ', but a lower bound value that underestimates the in situ friction angle by between 2° and 4°.

State parameter

The state parameter concept is a key element for describing the behaviour of granular soils, following the recognition that it combines the effects of both relative density and stress level. Mobilized friction, dilatancy and liquefaction susceptibility are all governed in some way by the state parameter.

Recent research based on the state parameter model (Yu, 1998) supports the view of K_D as an index reflecting the in situ state parameter Ψ. Although

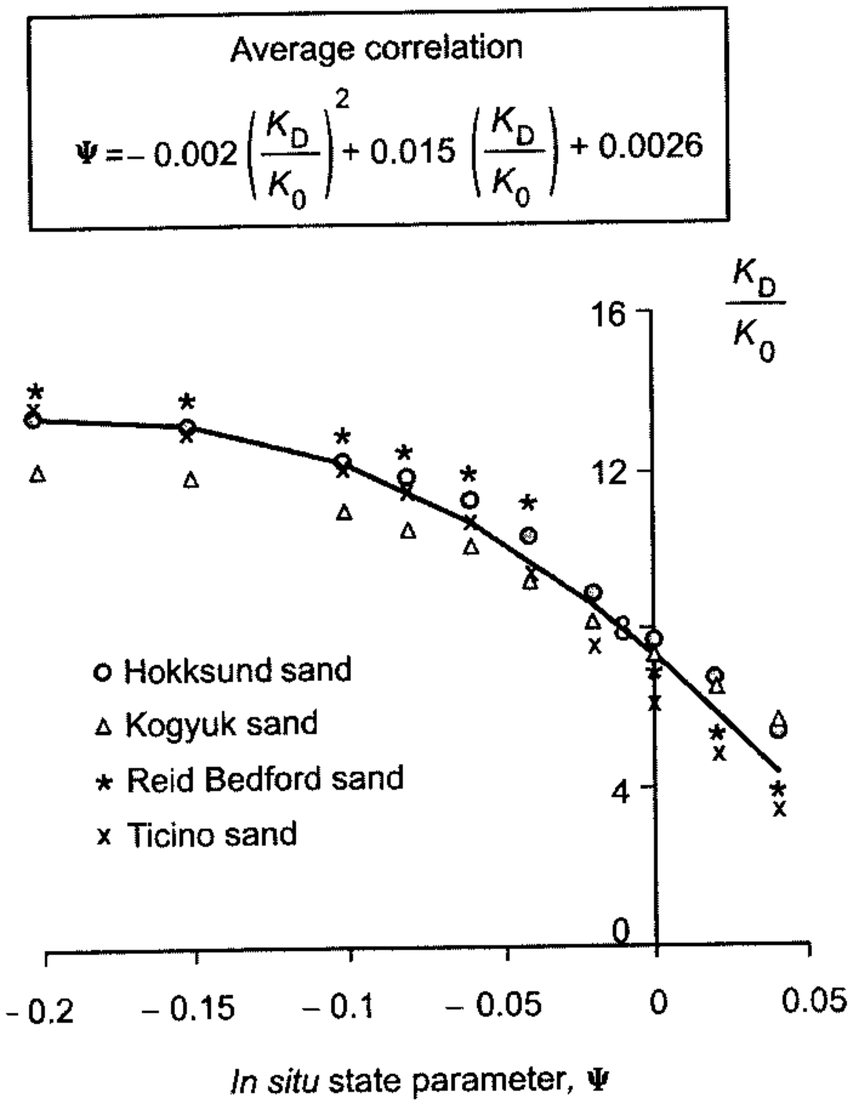

Figure 6.17 Average correlation for deriving the *in situ* state parameter from DMT (Yu, 2004).

K_D–Ψ correlations reflect the Cam clay constitutive parameters (Figure 6.17), for practical purposes Ψ can be estimated from the normalized dilatometer horizontal index K_D/K_0 using the following equation:

$$\Psi = -0.002\left(\frac{K_D}{K_0}\right)^2 + 0.015\left(\frac{K_D}{K_0}\right) + 0.0026 \qquad (6.16)$$

Soil stiffness

The small strain stiffness can be computed from the measured shear wave velocity and subsequently associated with operative strains representative of static loading conditions (see under Coefficient of consolidation above).

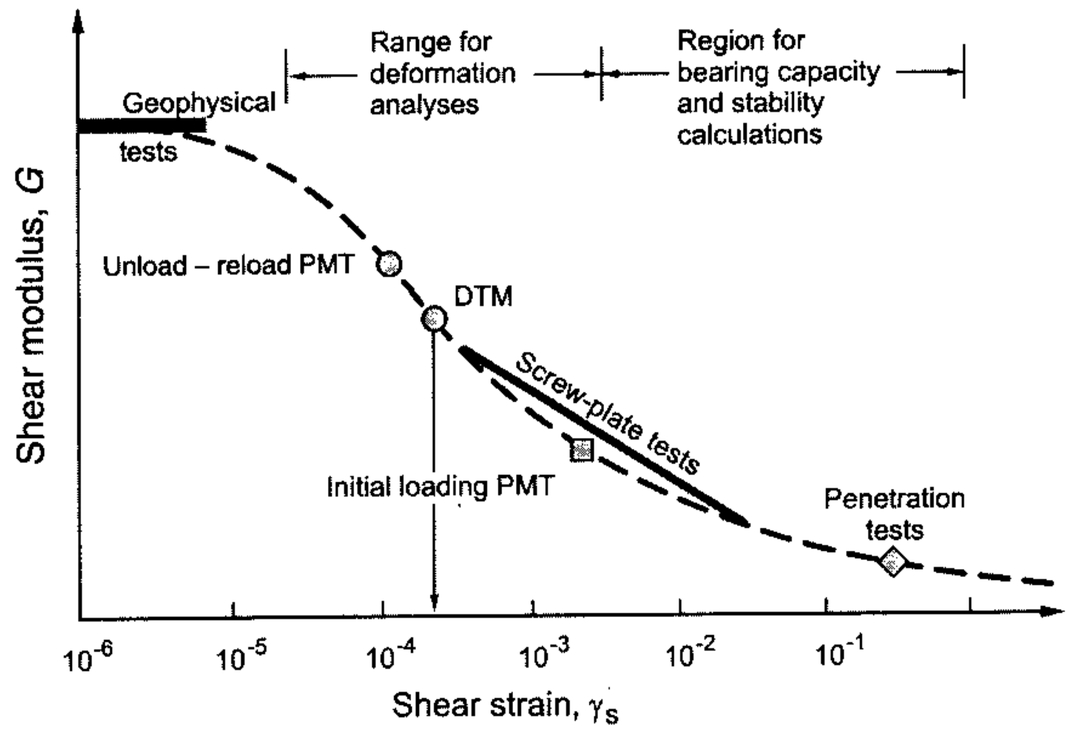

Figure 6.18 Decay of shear modulus with strain level and possible strain range of moduli from various *in situ* tests (Mayne, 2001).

This approach follows recent research efforts that are currently in progress to investigate the possible use of M_{DMT} for settlement predictions based on non-linear methods, taking into account the decay of soil stiffness with strain level using G–γ curves. Conceptually, the intention is to derive the in situ G–γ curve from two reference points: the initial shear modulus G_0 obtained from shear wave velocity v_s measurements and the M_{DMT} modulus at an operative strain. The M_{DMT} modulus is assumed to represent an intermediate strain level in the order of 0.05–0.1% (Mayne, 2001; Monaco *et al.*, 2006), as shown schematically in Figure 6.18.

In an alternative approach, research carried out in large laboratory calibration chamber tests has produced sound correlations for clean silica sand (Jamiolkowski *et al.*, 1988):

$$E'/E_D = 1.5 + 0.25 \text{ for normally consolidated} \qquad (6.17)$$

and

$$E'/E_D = 3.66 + 0.80 \text{ for overconsolidated} \qquad (6.18)$$

where the Young's modulus is defined at 0.1% axial strain.

Direct applications

Although geotechnical design should preferably be performed on the basis of sound analytical or numerical methods supported by constitutive parameters derived from both in situ and laboratory tests, DMT provides some useful additional applications for a wide range of practical problems, such as footing and pile design, anchored diaphragm walls, slope stability, liquefaction and sub-grade compaction control. Design of laterally loaded piles, establishing settlements of shallow foundations and assessing liquefaction are, in the author's view, the three most useful DMT applications.

Laterally loaded piles

The design of laterally loaded piles using the *p–y* approach was the original stimulus for the development of the flat dilatometer. In this approach, the *p–y* curve relates soil reaction to pile deflection as a means of representing the non-linear behaviour of the soil along the pile length. The two methods recommended for deriving the *p–y* curve are proposed by Robertson *et al.* (1987) and Marchetti *et al.* (1991).

Robertson *et al.* (1987) proposed a method that is an adaptation of early approaches, developed for estimating *p–y* curves from laboratory data (Matlock, 1970):

$$\frac{P}{P_u} = 0.5\left(\frac{y}{y_c}\right)^{0.33} \tag{6.19}$$

where P/P_u = ratio of soil resistance and y/y_c = ratio of pile deflection.

Input parameters are derived directly from the DMT. In clays, the value of pile deflection y_c is a function of the undrained strength, soil stiffness and in situ effective stress (after Skempton, 1951) and can be conveniently expressed as:

$$y_c = \frac{23.67 s_u D^{0.5}}{F_c E_D} \tag{6.20}$$

where y_c is in cm, D is the pile diameter in cm and F_c is taken as equal to 10 as a first approximation.

The evaluation of the ultimate static lateral resistance P_u is given by Matlock (1970) as:

$$P_u = N_p s_u D \tag{6.21}$$

where N_p is a non-dimensional ultimate resistance coefficient that can be expressed as:

$$N_p = 3 + \frac{\sigma'_{v0}}{s_u} + \left[J\frac{x}{D}\right] \tag{6.22}$$

where

$N_p \leq 9$
x = depth
σ'_{v0} = effective vertical stress at a given depth x
J = empirical coefficient equal to 0.5 for soft clay and 0.25 for stiff clay (Matlock, 1970).

In cohesionless soils, the reference pile deflection is calculated as a function of internal friction angle, effective vertical stress and pile diameter, as well as the dilatometer modulus:

$$y_c = \frac{4.17 \sin\phi' \sigma'_{v0}}{E_D(1 - \sin\phi')} D \tag{6.23}$$

where y_c and D are in cm. The ultimate lateral soil resistance P_u is determined by the following two equations (after Reese *et al.*, 1974; Murchison and O'Neill, 1984):

$$P_u = \sigma'_{v0}\left[D(K_p - K_a) + xK_p \tan\phi' \tan\beta\right] \tag{6.24}$$

$$P_u = \sigma'_{v0} D\left[K_p^3 + 2K_0 K_p^2 \tan\phi' + \tan\phi' - K_a\right] \tag{6.25}$$

where

σ'_{v0} = effective vertical stress at a given depth
D = pile diameter
ϕ' = internal friction angle

$K_a = \dfrac{1 - \sin\phi'}{1 + \sin\phi'}$ = Rankine active coefficient of earth pressure

$K_p = \dfrac{1 + \sin\phi'}{1 - \sin\phi'}$ = Rankine passive coefficient of earth pressure

K_0 = coefficient of earth pressure at rest
$\beta = 45° + \phi'/2$.

Values of ϕ' and K_0 can be estimated directly from DMT data and other in situ or laboratory tests.

Alternatively, Marchetti *et al.* (1991) developed a simple and effective method for deriving *p–y* curves in clay, which is based on a non-dimensional hyperbolic equation (Figure 6.19):

$$\frac{P}{P_u} = \tanh\left(\frac{E_{si} y}{P_u}\right) \tag{6.26}$$

with

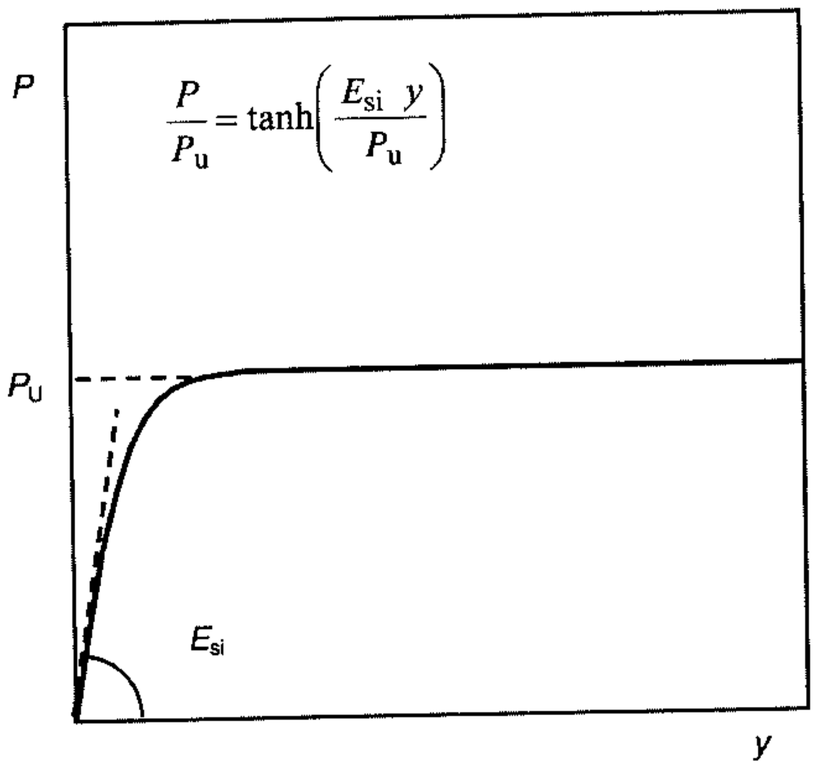

Figure 6.19 Hyperbolic representation of *p–y* curve (Marchetti *et al.*, 1991).

$$P_u = \alpha K_1 (p_0 - u_0) D \tag{6.27}$$

$$E_{si} = \alpha K_2 E_D \tag{6.28}$$

$$\alpha = \frac{1}{3} + \frac{2}{3}\frac{z}{7D} \leq 1 \tag{6.29}$$

where

E_{si} = initial soil modulus
α = non-dimensional reduction factor for depth $z < 7D$ (α becomes 1 for $z = 7D$)
p_0 = corrected first DMT reading
u_0 = in situ pore pressure
z = depth
K_1 = empirical coefficient of soil resistance (assumed as 1.24)
K_2 = empirical coefficient of soil stiffness: $K_2 = 10(D/0.5\text{m})^{0.5}$.

The two methods outlined above provide similar predictions and they are both fairly sensitive to changes in soil stiffness (Figure 6.20).

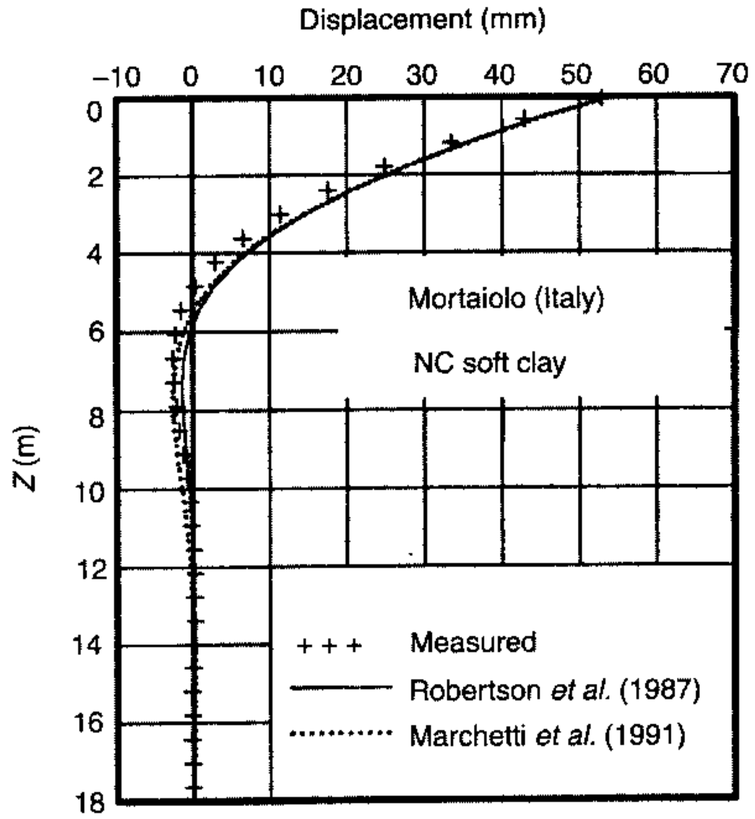

Figure 6.20 Comparison between measured and predicted displacement on laterally loaded pile (Marchetti *et al.*, 1991).

Settlement of shallow foundations

The DMT has proven to be a useful test in predicting settlements of shallow foundations in both sand and clay. Settlements are simply calculated as a one-dimensional problem (Figure 6.21):

$$S_{1DMT} = \sum \frac{\Delta\sigma_v}{M_{DMT}} \Delta z \tag{6.30}$$

where $\Delta\sigma_v$ is the stress increment calculated by Boussinesq and M_{DMT} is the constrained modulus estimated from DMT data (see above under Intermediate DMT parameters). Although, in theory, settlements can be calculated using one-dimensional (rafts) or three-dimensional (small isolated footings) formulae, Marchetti *et al.* (1991) suggested that the one-dimensional formula be used in all cases for DMT interpretation. This recommendation seems to be based on two considerations: first, the one-dimensional and the three-dimensional calculations generally give similar answers in most cases and, second, the emphasis given to DMT interpretation should be on the accurate determination of simple parameters, such as the one-dimensional compressibility coupled with simple calculations.

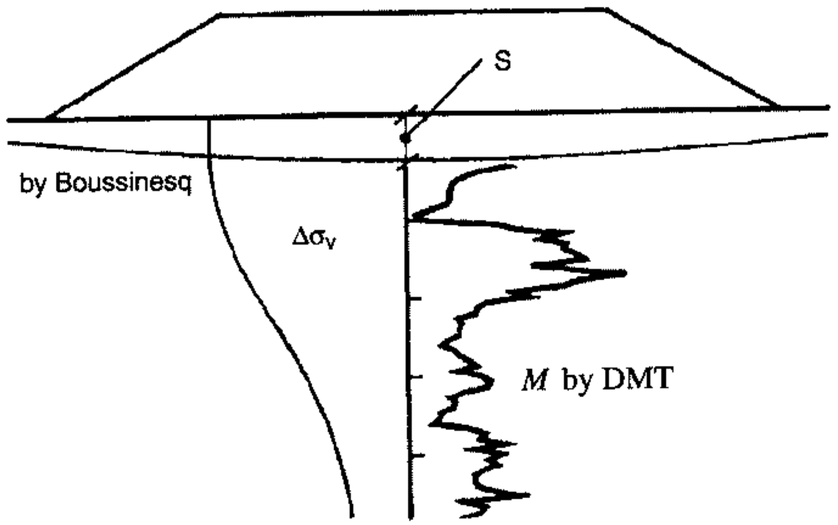

Figure 6.21 Recommended method for settlement calculation using DMT (Marchetti, 1997; Marchetti *et al.*, 2001).

This approach is particularly useful for clean uncemented sand where undisturbed samples cannot be retrieved. In addition, it can also be used as a first estimate of the primary settlement in clay with the M_{DMT} being treated as the average E_{oed} derived from the oedometer curve in the expected stress range.

Note that the settlement calculated from equation (6.30) is considered to be the settlement under *working conditions*, for a safety factor (SF) of about 3.0, since the M_{DMT} reflects an operative modulus that compares with moduli determined from back-calculations of shallow footings and rafts. A large number of documented case histories have confirmed this evidence by demonstrating that the elastic continuum solution from the dilatometer provides calculated settlements in line with the observed performance (Lacasse and Lunne, 1986; Schmertmann, 1986; Hayes, 1990; Woodward and McIntosh, 1993; Skiles and Townsend, 1994; Failmezger *et al.*, 1999; Pelnik *et al.*, 1999; Tice and Knott, 2000; Failmezger, 2001; Marchetti *et al.*, 2004; Mayne, 2005; Monaco *et al.*, 2006).

Schmertmann (1986) compiled measurements from 16 different locations and various soil types, including sand, silt, clay and organic soils with measured settlements ranging from 3 to 2,850 mm. The agreement observed between calculated and measured settlements is acceptable, with an average calculated/observed settlement ratio of 1.18, for ratios ranging from 0.7 to 1.3 and a standard deviation of 0.38 (Table 6.1). Monaco *et al.* (2006) updated Schmertmann's database to obtain a settlement ratio of ≈1.3 for footing sizes ranging from small footings to large rafts and embankments. Results summarized in Figure 6.22 demonstrate the generally satisfactory

Table 6.1 Comparison of DMT-calculated versus measured settlements from 16 case histories (Modified from Schmertmann, 1986)

Location	*Structure*	*Compressible soil*	*Settlement (mm)*		*Ratio DMT/measured*
			DMT	*Measured*	
Tampa	Bridge pier	Highly OC clay	25*	15	1.67
Jacksonville	Power plant (3 structures)	Compacted sand	15*	14	1.07
Lynn Haven	Factory	Peaty sand	188	185	1.02
British Columbia	Test embankment	Peat and organic soils	2,030	2,850	0.71
Fredricton	Surcharge	Sand	11*	15	0.73
"	3' plate load test	Sand	22*	28	0.79
"	Building (raft foundation)	Quick clayey silt	78*	35	2.23
Ontario	Road embankment	Peat	300*	275	1.09
"	Building	Peat	262*	270	0.97
Miami	4' plate load test	Peat	93	71	1.31
Peterborough	Apartment building	Sand and silt	58*	48	1.21
"	Factory	Sand and silt	20*	17	1.18
Peterborough	Water tank	Silty clay	30*	31	0.97
Linkoping	2 × 3 m plate	Silty sand	9*	6.7	1.34
"	1.1 × 1.3 m plate	Silty sand	4*	3	1.33
Sunne	House	Silt and sand	10**	8	1.25

* Ordinary method used (one-dimensional settlement, no adjustment of M for vertical effective stress during loading).

agreement between predicted and measured data, with the observed settlement falling within the range of ±50% from the DMT-predicted settlement.

Soil liquefaction

Procedures developed for estimating the liquefaction potential of soil deposits from the SPT and CPT have been reviewed in Chapters 2 and 3. These procedures are essentially supported by the early concepts developed by Seed and Idriss (1971), based on the cyclic shear stress ratios (*CSR*) induced by earthquake-generated ground motion (equation 2.68). The same concepts hold for

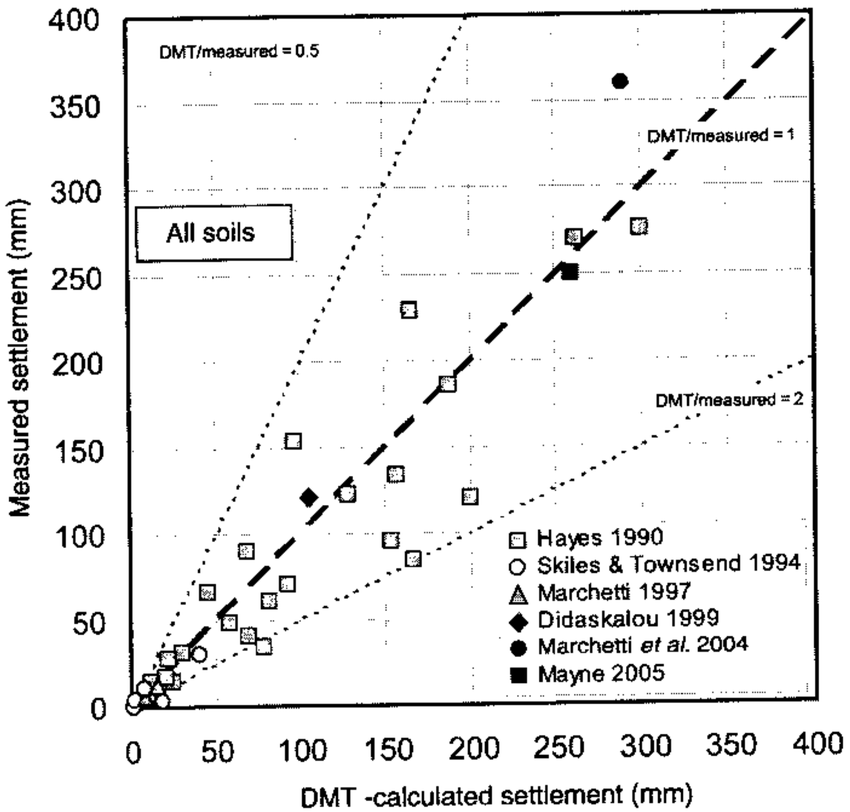

Figure 6.22 Summary of available comparisons of predicted versus observed settlements (Monaco et *al.*, 2006).

evaluation of seismic dilatometer liquefaction analysis methods, from which two parallel independent estimates of liquefaction resistance can be attained – one from K_D and one from v_s, using CRR–K_D and CRR–v_s correlations.

The use of v_s for evaluating CRR is acknowledged and has been described in Chapter 3 under the heading Liquefaction. Andrus and Stokoe (1997, 2000) present the derivation of a shear wave velocity dependent CRR for relatively small strains as a function of v_{s1} for magnitude $M_w = 7.5$ earthquakes.

The CRR–K_D correlations have been developed during the past two decades as an alternative to other in situ tests, prompted by the recognition of the sensitivity of K_D to stress history, aging, soil structure, cementation and relative density (Marchetti, 1982; Robertson and Campanella, 1986; Monaco *et al.*, 2005; Leon *et al.*, 2006; Maugeri and Monaco, 2006; Monaco and Marchetti, 2007; Monaco and Schmertmann, 2007). The ability of K_D to reflect the bonded structure in sand is a key element of the CRR–K_D correlation, since structure effect is considered to be a dominant factor controlling liquefaction behaviour.

The various methods developed to assess the liquefaction potential by differentiating between liquefiable and non-liquefiable soils are shown in

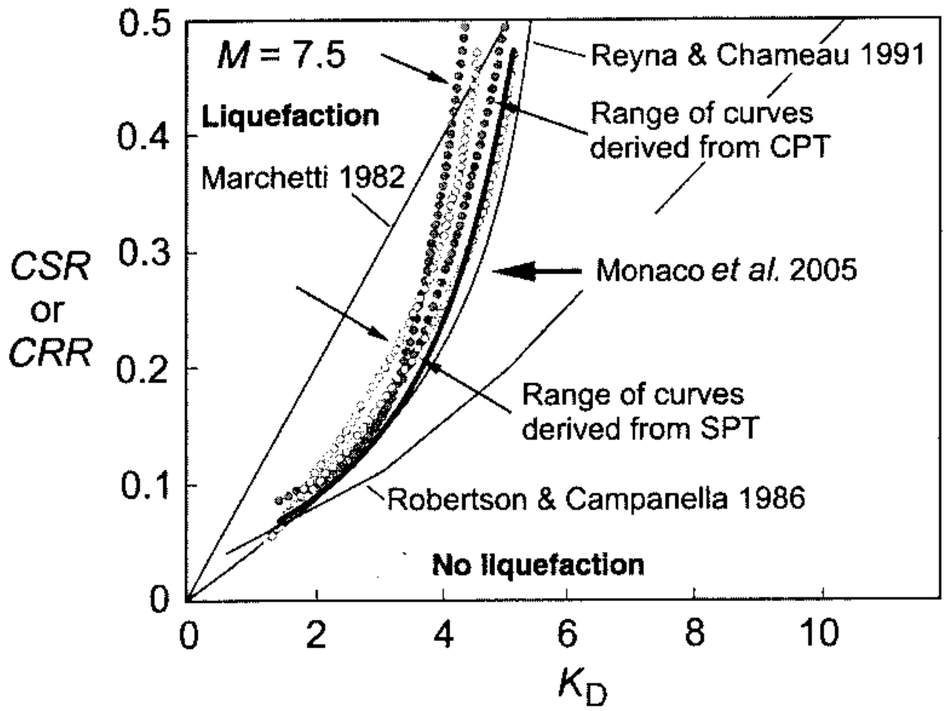

Figure 6.23 Tentative CRR–K_D correlation for evaluating liquefaction resistance from DMT (Monaco et *al.*, 2005).

Figure 6.23. The Robertson and Campanella (1986) and the Marchetti (1982) methods show substantial discrepancies. Based on expanded databases and on the re-evaluation of CPT and SPT-based procedures, the Reyna and Chameau (1991) and Monaco *et al.* (2005) methods produced more consistent predictions. These methods exhibit little divergence and can be used to evaluate the liquefaction potential of magnitude $M = 7.5$ earthquakes in clean sand. For magnitudes other than $M = 7.5$, magnitude scaling factors should be applied following recommendations given in Chapter 2 under the heading Soil liquefaction (after Idriss, 1999; Youd and Idriss, 2001).

The Monaco *et al.* (2005) method is presented in Figure 6.23 where liquefaction potential is identified in the CRR–K_D space. CRR is calculated as:

$$CRR_{7.5} = 0.0107K_D^3 - 0.0741K_D^2 + 0.2169K_D - 0.1306 \qquad (6.31)$$

More data should be gathered before using equation (6.31) with confidence. However, Marchetti and his co-workers emphasize the potential use of the CRR–K_D approach by pointing out that K_D is more sensitive than v_s in factors such as stress history and aging. OCR crusts (which are very unlikely to liquefy) are accurately depicted by K_D but are almost unfelt by v_s, which is suggestive of the lesser ability of v_s to profile liquefiability. In

addition, K_D is sensitive to both relative density and state parameter, which are known to greatly increase *CRR*.

Note

1 As discussed in Chapter 5, for a pressuremeter test in clean sand, the membrane deflates to its initial radius at approximately the equilibrium (hydrostatic) porewater pressure (e.g. Wroth, 1984). Campanella and Robertson (1991) reported data from a research dilatometer instrumented to measure pore pressure and the continuous deflection of the centre of the membrane. The authors observed remarkable similarities between the dilatometer and self-boring and full-displacement pressuremeter curves and concluded that, as the DMT membrane deflates, the sand arches and the C-reading closing pressure gives a measurement of u_0.